



# Energy Efficient Discontinuous Reception Strategy in LTE and Beyond Using an Adaptive Packet Queuing Technique

Bahram Rahmani

Faculty of Electrical and Computer Engineering, University of Tabriz, Tabriz, Iran,

**Abstract:** *The new generation of mobile communication systems is being developed for high-bandwidth mobile networks to accommodate the increasing demand for high data rate services like voice over IP, video streaming, and games. Due to high data rates, these applications drain the user equipment (UE) battery quickly. Long-Term Evolution (LTE)/LTE-advanced (A) has adopted a Discontinuous Reception (DRX) mechanism to improve the energy efficiency of a user equipment. DRX allows UEs to monitor the physical downlink control channel (PDCCH) discontinuously, when there is no downlink traffic for them, thus reducing their energy consumption. DRX results in higher latency due to its sleep cycle. In this paper, a new scheme was presented that could improve energy efficiency in UE, while maintaining average packet delay around a delay threshold. Numerical analysis and system simulation showed that this scheme was able to achieve significant power saving.*

**Keywords:** *Delay, DRX, LTE, Power Saving.*

## INTRODUCTION

LONG Term Evolution (LTE) is a standard for radio access technology designed by a collaboration of national and regional telecommunications standard bodies known as third Generation Partnership Project (3GPP), which is known as the 3GPP Long Term Evolution (Whinnett et al., 2013). The LTE standards aimed at supporting the growing user demands for high data rates and quality service as well as packet switch optimized system, which enhanced mobility. With increasing data rates and bandwidth, real-time applications, such as voice over IP, video and online gaming can be served into the network. These applications generate short packets every few second that substantially drain user equipment (UE) power (Fowle, Mellouk and Yamada, 2013).

The LTE standard specifies Discontinuous Reception mechanism (DRX) method to save UE's battery power through enabling the UE to turn off its RF circuitry when there is no downlink data packets (Bontu and Illidge, 2009). During this time, UE listens to the downlink channel less frequently, thus reduces power consumption significantly (Bontu and Illidge, 2009). With the DRX mechanism, the UE only wakes up periodically to listen to the Physical Downlink Control Channel (PDCCH), if there are no any data activities regarding UE's returning to the low power mode. DRX power saving is achieved at the expense of higher latency because all data packets of the UE that receive DRX sleep mode, must be buffered at the eNodeB until the time UE listens to the PDCCH (Bontu and Illidge, 2009).

In LTE networks, user equipment can be either in Radio Resource Control (RRC) IDLE or RRC CONNECTED

(Iwamura et al., 2010). The connected mode is enabled when UE is registered with an eNodeB or RRC CONNECTED. The IDLE mode or RRC IDLE state is enabled when no radio resources are allocated. In this state, UE is paged only for downlink traffic. In RRC CONNECTED state, RRC controls the sleep/active scheduling of each UE by configuring the following parameters: DRX inactivity timer, short DRX cycle, long DRX cycle and DRX short cycle timer (Iwamura et al., 2010).

These timers have significant impact on power saving and packet delay incurred by the UE's applications. If the UE follows a long inactivity timer or a short sleep cycle, it would remain in active state more time, thus less power would be saved. However, the delay would decrease. Therefore, a configuration mechanism is required to make an optimal tradeoff between power saving and delay time at the UEs.

In this paper, a new mechanism has been presented that improves the performance of the DRX technique and energy efficiency of the UEs. Proposed mechanism utilized packet delay, traffic rate and queue threshold in eNodeB, adjusted DRX inactivity timer to optimize energy consumption and maintained average packet delay around a given threshold. In this method, the well-known packet coalescing technique was used, as introduced in (Christensen et al., 2010), (Herreria-Alonso et al., 2012) and (Herrería-Alonso et al., 2015), which let eNodeB delay packet transmission to the UEs in DRX mode until their corresponding downlink queues reached a certain threshold. Regarding continuous reception mode (power active mode), DRX inactivity timer played an important role. It determined how long UE must remain active (ON) when there was no any scheduled packet for it after monitoring PDCCH. In the proposed algorithm, DRX inactivity timer dynamically adapted to traffic rate and queue threshold, in this way when there was no downlink data packets for UE (low traffic rate), inactivity timer would be decreased to reduce energy consumption, and when traffic rate was high, inactivity timer would be increased to reduce packet delay. The performance of proposed algorithm in terms of energy consumption in the UE and average packet delay has been studied for two types of traffic. Regarding background traffic, Poisson model was used and for self-similar internet traffic, Pareto model was utilized.

The rest of this paper has been organized as follows: Section 1 has presented the relevant background and related works. Section 2 has described the DRX mechanism in LTE network. Proposed DRX algorithm has been detailed in section 4. Simulations results have been presented in section 3 and concluding remarks have been appeared in section 4.

## 1. Background and Related Work

The principal purpose of DRX is to extend UE's battery lifetime (Fowle, Mellouk and Yamada, 2013). The DRX mechanism is based on a simple principle; when there is no transmission data, UE would switch to sleep mode to save power (Fowle, Mellouk and Yamada, 2013). Adjustable DRX mechanism was investigated in (Liu et al., 2014), in which DRX short and long cycles have been adjusted using two parameters  $a$  and  $\beta$ . The authors showed by choosing  $a = 1$  and  $\beta = 2$  in adjustable DRX mechanism that the wake-up delay decreased by approximately 66.7 % for the case that DRX short sleep period equaled to 200ms. The smaller values of  $a$  and  $\beta$  are suggested for delay sensitive applications, while larger values of  $a$  and  $\beta$  are more suitable for applications such as background traffic and social networking. The limitation of this method was that  $a$  and  $\beta$  remained constant during DRX cycle regardless of traffic condition and packet delay and thus its efficiency was reduced.

A trade-off relationship between power saving and wake up delay was investigated in (Zhong et al., 2011). When the UE turned off its circuits, the next packet delivery did not happen until the UE returned to the active mode. The effect of Transmission Time Interval (TTI) on DRX mechanism for Voice and Web traffic have been studied in (Fowler, 2011). In this study, an optimal TTI parameter was figured out for maximum power efficiency with minimum delay. A traffic-based scheme has been proposed to enhance energy saving performance in UE (Yu and Feng, 2012). A partially observable Markov decision process (POMDP) was employed to conjecture the present traffic status. Optimal DRX parameters can be obtained via the POMDP

framework. In (Aho et al., 2009) the performance of the DRX mechanism was evaluated in terms of DRX cycle lengths and related timer values, by observing their effect on VoIP traffic service over the High Speed Downlink Packet Access (HSDPA) network. The results showed that a longer DRX cycle saved more power, but, at the same time, VoIP capacity over HSDPA can be compromised in the case when no suitable selection of DRX parameters was applied.

The trade-off between the power saving and the queuing delay in LTE/LTE-A radio devices with Discontinuous Reception (DRX) Mechanism has been discussed in (Ramazanali and Vinel, 2016). Two optimization problems to tune the DRX parameters were formulated in this study. Dynamic and Adjustable DRX (DADRX) mechanism were proposed in (Ferng and Wang, 2018). The proposed algorithm extended the number of sleep cycles in original DRX with additional types of sleep cycles. To this end, two types of DADRX have been proposed. First algorithm could control the level of expanding DRX cycles by adding different pairs of sleep cycles with different sleep periods and in the second algorithm the total numbers of types of sleep were fixed, but further employed a set of level expanding probabilities to probabilistically control the possible pairs of sleep cycles that can be reached.

DRX for Machine-type Communications in LTE-A networks has been proposed in (Chang and Tsai, 2018). The standard DRX was designed for normal mobile users. In this paper, authors proposed optimistic DRX (ODRX) mechanism as suitable for MTC devices. In (Lee and Lee, 2017), the authors proposed a novel DRX mechanism in wireless powered cellular networks (WPCNS) that focused on an IoT device with energy harvesting capability. In this paper short DRX cycles were optimized based on the harvested energy and the consumed energy on the IoT device.

The effective DRX mechanism for 5G communications has been proposed in (Maheshwari et al., 2017). The authors proposed Hybrid Directional DRX (HD-DRX) mechanism when beam searching was performed. In HD-DRX mechanism, dual radio in UE received incoming packets from eNodeB and performed beam search only when necessary. The standard DRX mechanism provided by 3GPP was inadequate to the narrowband Internet of Things (NB-IoT). In (Xu, Liu and Zhang, 2018) Shaoyi Xu et al. proposed a grouping based DRX mechanism for NB-IoT radio technology, which devised the different DRX schemes for the group leader and the group members.

The proposed algorithm in this paper adjusted DRX inactivity timer based on the number of packets in queue and traffic conditions by queuing packets in eNodeB. With these parameters, the proposed algorithm acquired the maximum amount of the power saving. In this model, if packet delay exceeded from the threshold delay, DRX inactivity timer dynamically decreased, so the packet delay could be always under control. According to this study's analytical and simulations results, the proposed algorithm maximized the power saving, adaptively modified the DRX inactivity timer in terms of traffic rate and queue threshold, controlled the packet delay by considering the delay threshold, and exhibited high performance in different traffic scenarios compared to other DRX schemes.

## 2. The DRX Mechanism In LTE

Discontinuous Reception (DRX) is a power saving technique in UE. Simply put, it switches off the receiver and puts the device into power-saving mode, when it is not in use. The basic DRX mechanism works as follows: Each UE is assigned a periodic wake (ON) period for monitoring PDCCH. It wakes up immediately when uplink/downlink traffic arrives before it enters to DRX sleep state. On the other hand, UE turns its receiver off and goes into power-saving mode (DRX sleep mode) until the next periodic wake period (Fowle, Mellouk and Yamada, 2013). With this technique, power consumption at UE would be reduced and UE's battery lifetime would be extended. In DRX, downlink data transfer happens only during awake (ON) time. Therefore, the trade-off between power saving and delay is an important factor when applying the DRX cycle efficiently. In RRC CONNECTED state, the base station configures a UE's DRX parameters by the means of RRC signaling. RRC controls the sleep/wake scheduling of each UE by configuring the following parameters:

ON duration timer ( $t_{ON}$ ), DRX inactivity timer ( $t_I$ ), short DRX cycle ( $t_{DS}$ ), long DRX cycle ( $t_{DL}$ ) and DRX short cycle timer ( $t_N$ ) (Fowle, Mellouk and Yamada, 2013). The DRX parameters are illustrated in Fig. 1. The details of the parameters are explained as follows:

**DRX inactivity timer ( $t_I$ ):** It defines how long UE must remain active when UE finds out that there are no downlink packets after periodic monitoring of PDCCH. DRX inactivity timer is also reset with any uplink/downlink data activities. When this timer expires, UE stays in connected state but moves to DRX mode.

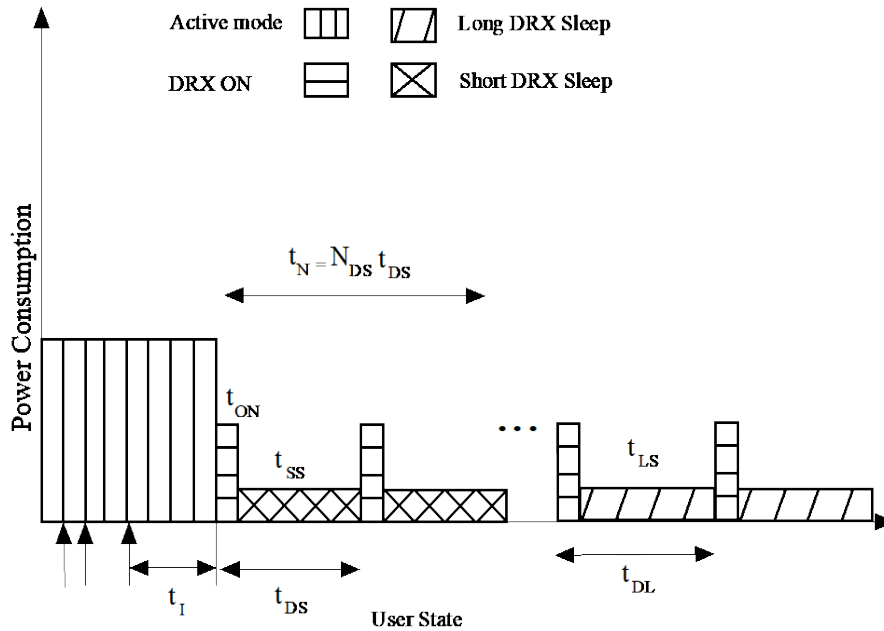


**Figure 1.** 3GPP DRX mechanism in LTE.

**ON duration timer ( $t_{ON}$ ):** It is periodic awake for detecting any data activities, and UE monitors PDCCH for downlink data reception. Once data activities are detected, UE wakes up and DRX inactivity timer ( $t_I$ ) is activated. The duration of ( $t_{ON}$ ) is consistent between short and long DRX cycle.

**short DRX cycle ( $t_{DS}$ ):** Upon the expiry of ( $t_I$ ), UE enters in short DRX cycle. It consists of a short sleep-duration plus one ON duration period.

**DRX short cycle timer ( $t_N$ ):** It defines how many short DRX cycle should be repeated before it transits into deep sleep mode.

**long DRX cycle ( $t_{DL}$ ):** Upon the expiry of ( $t_N$ ), UE enters into long DRX cycle. It consists a long sleep-duration plus one ON duration period.

The UE powers down most of its circuitry either in short sleep or long sleep state, thus it consumes much lower battery resource when compared to continuous reception state and DRX ON state. The parameters of DRX configuration can be optimized to either maximize power saving or minimize packet latency in UE. Short DRX cycle is desirable for delaying sensitive applications such as voice over IP and video streaming, as it reduces overall latency. For some other applications, such as background traffic and social networking, long DRX cycle for power efficiency is more preferable.

According to the above statements, a configuration of The DRX parameters to achieve the best tradeoff between power saving and delay is critical at the UE's.

### 3. The Proposed DRX Mechanism

#### A. Traffic model

Studies have shown that for some environments, the traffic data are self-similar (Willinger et al., 1997). With self-similar traffic, it displays burstiness and interacts over an immensely wide range of time scales, making it long range dependent. In addition, it has been shown to be heavy tailed such as Pareto. Since Weibull distributions are more applicable when modeling data network traffic (Yang, Yan and Hung, 2007). In the current paper, European Telecommunication Standards Institute (ETSI) bursty packet data traffic model has been adapted for Analytical computations. Where the statistical distribution of the bursty packet data parameters are summarized in Table 1. A new packet call can be considered as the continuation of the current session (case 1) or as the onset of a new session (case 2) depending on the interval-arrive time between two consecutive packet calls. The packet calls may be the interpacket call idle time ( $t_{ipc}$ ) with the probability of  $P_{pc} = 1 - 1/\mu_{pc}$  or the intersession idle time ( $t_{is}$ ) with probability of  $P_s = 1/\mu_{pc}$ . The probabilities take into account the memoryless property of geometric distributions.

**Table 1:** Distribution of Bursty Packet Data Parameters

Parameter	Distribution	Mean value
Intersession idle time ( $t_{is}$ )	Exponential	$1/\lambda_{is}$
Number of packets calls per session ( $N_{pc}$ )	Geometric	$\mu_{pc}$
Inter-packet call idle time ( $t_{ipc}$ )	Exponential	$1/\lambda_{ipc}$
Number of packet calls per packet call ( $N_p$ )	Geometric	$\mu_p$
Inter-packet arrival time ( $t_{ip}$ )	Exponential	$1/\lambda_{ip}$

The proposed mechanism of this study utilized application's delay sensitivity and traffic rate to modify DRX inactivity timer ( $t_I$ ) adaptively. In this method, the Adaptive Coalesced DRX mechanism has been used that has been introduced in (Christensen et al., 2010), (Herreria-Alonso et al., 2012) and (Herrería-Alonso et al., 2015). EnodeB in Coalesced DRX mechanism delays packet transmission to the UEs in DRX mode until their corresponding downlink queues reach a certain threshold ( $Q_{th}$ ), since the single queue threshold value does not suit well for any traffic rate, in adaptive coalesced DRX mechanism queue threshold adaptively adjusts to real time traffic with the goal of maintaining average packet delay around a given target, while keeping energy consumption low enough.

In continuous reception mode (inactive DRX), DRX inactivity timer ( $t_I$ ) plays an important role. It determines how long UE must remain active (ON), when there is no scheduled packets for it after monitoring PDCCH. There are two possible scenarios in power active modes. First it may be that as packets arrive, UE processes them. In this case, after a successful reception on the PDCCH, DRX inactivity timer  $t_I$  is re-initiated for another round and UE stays ON. In the other cases, there is no any packet arriving before ( $t_I$ ) has expired, in this case,  $t_I$  will be eventually expired and the UE would transit into short sleep mode. The probability that new packet call begins before expiration of DRX inactive timer is:

$$P = P_r[t_{ipc} < t_I] + P_r[t_{is} < t_I] = P_{pc}(1 - e^{-\lambda_{ipc}t_I}) + P_s(1 - e^{-\lambda_{is}t_I}) \quad (1)$$

According to the (1), it is clear that changes in  $t_I$  makes the UE sooner or later go to the sleep mode, which has direct effect on power saving and latency. Since the goal is reducing power consumption in UE for when there is no scheduled packets for UE (low traffic rate) and reducing latency for when a large number of packets are in queue to be received. Therefore, if traffic rate is low the  $t_I$  must be decreased to the UE quickly, to go into sleep mode and if traffic rate is high the  $t_I$  must be increased to decrease packet delay.

### B. Adaptive algorithm

To obtain the highest energy saving, the DRX inactivity timer should be adjusted based on traffic rate and the queue threshold. The  $t_I$  has been defined as follows:

$$t_I = \alpha Q_{th} + \beta \lambda \quad (2)$$

Where  $\alpha$  and  $\beta$  are constant factors depending on application's sensitivity to delay.  $\lambda$  is traffic rate that is  $0 \leq \lambda \leq 0.9$  for Poisson and Pareto traffic model.  $Q_{th}$  is queue threshold in eNodeB. To adjust the  $Q_{th}$  parameter to traffic rate, Algorithm 1 was used that dynamically accommodated queue threshold to incoming traffic. It is introduced in (Herrería-Alonso et al., 2015). To adjust the  $Q_{th}$  parameter to the existent traffic conditions, the average delay experienced by packets in a given coalescing cycle  $i$ , that is,  $D[i]$ , should be measured and compared with the target delay  $D_{th}$ . Then, if  $D[i] > D_{th}$ ,  $Q_{th}$  should be reduced to diminish packet delay. Conversely, if  $D[i] < D_{th}$ , current average packet delay would be low enough and  $Q_{th}$  can be increased to reduce power consumption (Herrería-Alonso et al., 2015).

<b>Algorithm 1</b> : Tunning $Q_{th}$	
D[i]:	the average delay in current cycle i
1:	$Q_{th}[i + 1] = Q_{th}[i] + 2\lambda(D_{th} - D[i])$
2:	if ( $Q_{th}[i + 1] \leq 1$ ) Then
3:	$Q_{th}[i + 1] = 1$
4:	else if ( $Q_{th}[i + 1] > Q_{max}$ ) Then
5:	$Q_{th}[i + 1] = Q_{max}$
6:	end if

When traffic rate is low (low  $\lambda$ ),  $Q_{th}$  decreases to diminish packet delay. So, by reducing  $A$  and  $Q_{th}$ ,  $t_I$  also decreases and the UE sooner goes to sleep mode (DRX mode) to increase power saving in the UE. When traffic rate is high (high  $\lambda$ ), since the queue should be stuffed quickly,  $Q_{th}$  increases. So, by increasing  $\lambda$  and  $Q_{th}$ ,  $t_I$  also increases to the UE goes to sleep mode later, so the delay decreases. Therefore, in low traffic load more power is saved and in high traffic load, delay does not increase too much. Since a threshold delay ( $D_{th}$ ) is considered to maintain the average packet delay around threshold delay for when  $Q_{th}$  is increasing, it was assured that by decreasing  $t_I$  in low traffic load, average packet delay would not exceed form the ( $D_{th}$ ). Also note that, in Algorithm 1,  $Q_{th}$  must not exceed a maximum value  $Q_{max} = D_{max}/t_s$ , where  $t_s$  is the maximum service time a packet could demand, to avoid introducing queueing delays greater than  $D_{max}$ . To obtain optimal values of  $a$  and  $\beta$  for maintaining average packet delay around a given target and maximize power saving, we should get expression for power saving factor and average queueing delay.

### C. Semi-Markov Process

The LTE DRX mechanism is a semi-Markov process and four states constitute the semi-Markov process which is depicted in Fig. 2 (Ross, 1996). We describe it to consider the power saving and delay as the two performance metrics. Based on the DRX operation described in Section 2, the UE can be in one of the following four states:

- 1) State  $S_1$ : This is continuous reception state and highest power consumption is in this state because of most active in transmitting or receiving data and or monitoring PDCCH. The inactivity timer after receiving a packet will be reset and if there are no data activities for a period of  $t_I$ ,  $t_I$  would expire and UE would move to the state  $S_2$ .
- 2) State  $S_2$ : DRX ON state ( $t_{ON}$ ). After the expiry of  $t_I$ , UE moves into  $S_2$ . Also, at the end of DRX sleep cycle, UE moves into  $S_2$ . In this state UE listens to PDCCH if a new packet arrives before  $t_{ON}$  expires then UE moves to  $S_1$ . Otherwise, at the end of  $t_{ON}$  UE moves to either  $S_3$  or  $S_4$ . UE moves to  $S_4$  only if DRX short cycle timer ( $t_N$ ) expires. During  $t_{ON}$ , UE does not receive or transmit data; however, it

monitors PDCCH. Power consumption in this state is less than state  $S_1$  but is more than state  $S_3$  and state  $S_4$ .

- 3) State  $S_3$ : DRX short sleep cycle ( $t_{ss}$ ). In this state, UE turns off its transceiver, thus its power consumption is close to zero. The arrived packet data of this state, will be buffered until the next DRX ON state. After DRX short cycle expires, UE moves to state  $S_2$ .
- 4) State  $S_4$ : DRX long sleep cycle ( $t_{ls}$ ). After  $t_{ON}$  and expiry of  $t_N$ , UE enters to this state. Similar to  $S_3$ , UE turns off its transceiver thus its power consumption is close to zero. The packet data arrives in this state will be buffered until the next DRX ON state.

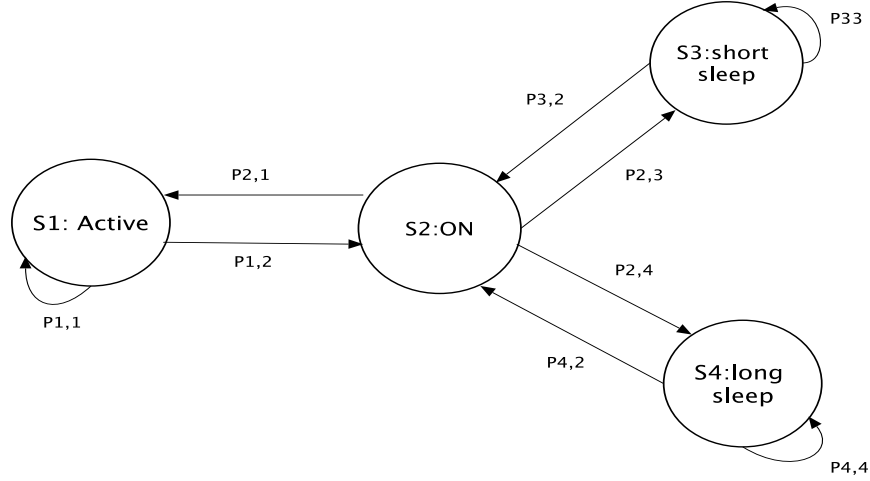


**Figure 2.** Four-State Semi-Markov Process for DRX Mechanism.

#### D. Power saving factor and Delay analysis

Here we analytically compute the power saving factor and average packet delay of DRX mechanism for when eNodeB buffers packet until the number of packets in queue reach to  $Q_{th}$  packets. The basics of mathematical analysis that have been used to compute the power saving factor are based on (Fowle, Mellouk and Yamada, 2013) and (Liu et al., 2014), the first reference introduces mathematical analysis and performance evaluation of power-saving mechanisms in 3GPP LTE and LTE-Advanced networks. The transition probabilities for the Markov chain are shown in Fig. 2, where  $P_{m,n} \forall n, m \in \{1, 2, 3, 4\}$  represent the transition probability from state  $n$  to  $m$ . The percentage of time that UE spends in sleeping mode is the indicator of the power saving performance that the DRX mechanism achieves. Thus, to get the expression for power saving factor and average packet delay, calculating the transition probabilities and the amount of time that UE spends in sleep mode is necessary.

- 1) State  $S_1$ : In this state, it was assumed that if a packet arrives in eNodeB, it should be immediately transmitted without requiring to be buffered, where there is no difference between conventional state  $S_1$  DRX. When UE is in state  $S_1$ , if the next packet call starts before the expiry of  $t_1$ , UE restarts  $t_1$  and stays in this state, otherwise moves to  $S_2$ . The probability that a new packet call arrives before the expiration of  $t_1$  in case 1 (continuation of the current session) is:

$$q_1 = P_r[t_{ipc} < t_1] = \int_0^{t_1} \lambda_{ipc} e^{-\lambda_{ipc}t} dt = 1 - e^{-\lambda_{ipc}t_1} \quad (3)$$

and the probability that a new packet call arrives before expiration of  $t_1$  in case 2 (new session) is:

$$q_2 = P_r[t_{is} < t_1] = \int_0^{t_1} \lambda_{ipc} e^{-\lambda_{is}t} dt = 1 - e^{-\lambda_{is}t_1} \quad (4)$$

Therefore,  $P_{1,1}$  and  $P_{1,2}$  can be computed as follow:

$$P_{1,1} = P_{pc}q_1 + P_s q_2 \quad (5)$$

$$P_{1,2} = P_{pc}(1 - q_1) + P_s(1 - q_2) \quad (6)$$

- 2) State  $S_2$ : In this state it was assumed that UE goes to the active state ( $S_1$ ) when downlink queue in eNodeB reaches a certain tunable threshold ( $Q_{th}$ ). Otherwise, at the end of the  $t_{ON}$ , it goes to  $S_3$  or  $S_4$ . UE goes to  $S_4$  only if it has been in  $S_3$  for  $N_{DS}$  times, consecutively. The probability that downlink queue in eNodeB reaches  $Q_{th}$  packets before expiration of  $t_{ON}$  in case 1 is:

$$q_3 = P_r[t_{ipc} < t_{ON}] = \int_0^{t_{ON}} f_{Q_{th}}(t_{ipc} = t)dt \quad (7)$$

and the probability that downlink queue in eNodeB reaches  $Q_{th}$  packets before expiration of  $t_{ON}$  in case 2 is:

$$q_4 = P_r[t_{is} < t_{ON}] = \int_0^{t_{ON}} f_{Q_{th}}(t_{is} = t)dt \quad (8)$$

The probability that downlink queue in eNodeB reaches  $Q_{th}$  packets before DRX short cycle timer ( $t_N$ ) expires in case 1 is:

$$q_5 = P_r[t_{ipc} < t_N] = \int_0^{t_N} f_{Q_{th}}(t_{ipc} = t)dt \quad (9)$$

The probability that downlink queue in eNodeB reaches  $Q_{th}$  packets before DRX short cycle timer ( $t_N$ ) expires in case 2 is:

$$q_6 = P_r[t_{is} < t_N] = \int_0^{t_N} f_{Q_{th}}(t_{is} = t)dt \quad (10)$$

Therefore,  $P_{2,1}$ ,  $P_{2,3}$  and  $P_{2,4}$  can be computed as:

$$P_{2,1} = P_{pc}q_3 + P_s q_4 \quad (11)$$

$$P_{2,3} = P_{pc}(1 - q_3)q_5 + P_s(1 - q_4)q_6 \quad (12)$$

$$P_{2,3} = P_{pc}(1 - q_3)(1 - q_5) + P_s(1 - q_4)(1 - q_6) \quad (13)$$

Where  $f_{Q_{th}}(t)$  is the probability density function of arriving  $Q_{th}$  packets in eNodeB. Generally, there is no simple closed form for this function, since it was assumed that interarrival packet times ( $I_n$ ) are independent, so we can get:

$$f_{Q_{th}}(t_{is}) = f_{I_1}(t) * f_{I_2}(t) * \dots * f_{Q_{th}}(t) \quad (14)$$

where  $*$  is the convolution operator. In standard ETSI traffic model interarrival packet times are exponentially distributed. Therefore, the arrival time of the  $Q_{th}$  packets is Erlang-  $Q_{th}$  distributed:

$$f_{Q_{th}}(t_{is}) = \lambda^{Q_{th}} t^{Q_{th}-1} \frac{e^{-\lambda t}}{(Q_{th}-1)!} \quad (15)$$

Then the probabilities of  $P_{2,1}$ ,  $P_{2,3}$  and  $P_{2,4}$  can be calculated.

- 3) State  $S_3$ : After expiration of  $t_{ON}$ , UE goes to state  $S_3$  or state  $S_4$ . First  $N_{DS}$  expiry of  $t_{ON}$ , UE moves to  $S_3$  and then after any expiry of  $t_{ON}$ , UE moves to  $S_4$ . The UE stays in state  $S_3$  even if a new packet call



arrives, so we have:

$$q_7 = P_r[t_{ipc} > t_{SS}] = \int_{t_{SS}}^{\infty} \lambda_{ipc} e^{-\lambda_{ipc}t} dt = e^{-\lambda_{ipc}t_{SS}} \quad (16)$$

and for case 2 we have:

$$q_8 = P_r[t_{is} > t_{SS}] = \int_{t_{SS}}^{\infty} \lambda_{ipc} e^{-\lambda_{is}t} dt = e^{-\lambda_{is}t_{SS}} \quad (17)$$

Therefore,  $P_{3,2}$  and  $P_{3,3}$  can be computed as:

$$P_{1,1} = P_{pc}q_1 + P_sq_2 \quad (18)$$

$$P_{1,2} = P_{pc}(1 - q_1) + P_s(1 - q_2) \quad (19)$$

4) State  $S_4$ : Similarly, we can compute:

$$q_9 = P_r[t_{ipc} > t_{LS}] = \int_{t_{LS}}^{\infty} \lambda_{ipc} e^{-\lambda_{ipc}t} dt = e^{-\lambda_{ipc}t_{LS}} \quad (20)$$

and for case 2 we have:

$$q_{10} = P_r[t_{is} > t_{LS}] = \int_{t_{LS}}^{\infty} \lambda_{is} e^{-\lambda_{is}t} dt = e^{-\lambda_{is}t_{LS}} \quad (21)$$

Therefore,  $P_{4,2}$  and  $P_{4,4}$  can be computed as:

$$P_{4,2} = P_{pc}q_9 + P_sq_{10} \quad (22)$$

$$P_{4,4} = P_{pc}(1 - q_9) + P_s(1 - q_{10}) \quad (23)$$

The transition probability matrix  $\mathbf{P} = (P_{i,j})$  of the Markov chain can be also obtained as:

$$\mathbf{P} = \begin{bmatrix} P_{1,1} & P_{1,2} & 0 & 0 \\ P_{2,1} & 0 & P_{2,3} & P_{2,4} \\ 0 & P_{3,2} & P_{3,3} & 0 \\ 0 & P_{3,2} & 0 & P_{4,4} \end{bmatrix} \quad (24)$$

Let  $\pi_i$  ( $i \in \{1, 2, 3, 4\}$ ) denote the probability that the Markov chain is in state  $S_i$  ( $i \in \{1, 2, 3, 4\}$ ). By using  $\sum_{i=1}^4 \pi_i = 1$  and the balance equation  $\pi_i = \sum_{j=1}^4 \pi_j P_{j,i} = 1$ , the expressions for steady state probabilities can be obtained as:

$$\pi_1 = \frac{P_{2,1}(1 - P_{3,3})(1 - P_{4,4})}{\Delta} \quad (25)$$

$$\pi_2 = \frac{(1 - P_{1,1})(1 - P_{3,3})(1 - P_{4,4})}{\Delta} \quad (26)$$

$$\pi_3 = \frac{P_{2,3}(1 - P_{3,3})(1 - P_{4,4})}{\Delta} \quad (27)$$

$$\pi_4 = \frac{P_{2,4}(1 - P_{3,3})(1 - P_{4,4})}{\Delta} \quad (28)$$

Where  $\Delta = (1 - P_{1,1})(1 - P_{3,3})(1 - P_{4,4}) + P_{2,1}(1 - P_{3,3})(1 - P_{4,4}) + P_{2,3}(1 - P_{1,1})(1 - P_{4,4}) + P_{2,4}(1 - P_{3,3})(1 - P_{1,1})$ .

After computing steady state probabilities, in order to get power saving factor. It was needed to get mean holding time in each state. Let  $H_i$  ( $i \in \{1, 2, 3, 4\}$ ) represent the holding time of the Markov process at state  $S_i$  ( $i \in \{1, 2, 3, 4\}$ ). The expected value  $E[H_i]$  of the holding time of different states can be obtained.

- 1)  $E[H_1]$ : The mean holding time in state  $S_1$  contains the total service time for the number of packets within a packet call and then an inter-packet call inactivity period  $\overline{t_l}$  (Klenrock, 1975). We can have:

$$E[H_1] = E[T_{service}] + \overline{E[t_l]} \quad (29)$$

Since a service time is identical to the duration of a packets call delivery, a  $T_{service}$  consists of  $N_p$  packets service times  $t_{service}$ :

$$E[T_{service}] = E[N_p]E[t_{service}] = \frac{\mu_p}{\lambda_s} \quad (30)$$

where  $\mu_p$  is the number of packet calls within a packet service session and  $\frac{1}{\lambda_s}$  is the mean of service time. If a packet arrives before the inactivity timer expires ( $t_{ipc} < t_l$ ), then  $\overline{t_l} = t_{ipc}$ ; otherwise, the next packet arrives after the inactivity timer has expired ( $t_{ipc} > t_l$ ), then  $\overline{t_l} = t_l$ . Therefore, we have  $\overline{t_l} = \min(t_{ipc}, t_l)$ . So, we have (Fowle, Mellouk and Yamada, 2013):

$$E[\overline{t_l}] = P_{pc}E[\min(t_{ipc}, t_l)] + P_sE[\min(t_{is}, t_l)] \quad (31)$$

where:

$$\begin{aligned} E[\min(t_{ipc}, t_l)] &= \int_{x=0}^{\infty} P_r[\min(t_{ipc}, t_l) > x]dx \\ &= \int_{x=0}^{t_l} P_r[t_{ipc} > x]dx \\ &= \int_{x=0}^{t_l} e^{-\lambda_{ipc}x} dx \\ &= \frac{1}{\lambda_{ipc}} [1 - e^{-\lambda_{ipc}t_l}] \end{aligned} \quad (32)$$

Similarly:

$$\begin{aligned} E[\min(t_{is}, t_l)] &= \int_{x=0}^{\infty} P_r[\min(t_{is}, t_l) > x]dx \\ &= \int_{x=0}^{t_l} P_r[t_{is} > x]dx \\ &= \int_{x=0}^{t_l} e^{-\lambda_{is}x} dx \\ &= \frac{1}{\lambda_{is}} [1 - e^{-\lambda_{is}t_l}] \end{aligned} \quad (33)$$

Substitute (32) and (33) into (31):

$$E[\overline{t_l}] = \frac{P_{pc}}{\lambda_{ipc}} [1 - e^{-\lambda_{ipc}t_l}] + \frac{P_s}{\lambda_{is}} [1 - e^{-\lambda_{is}t_l}] \quad (34)$$

And finally:

$$E[H_1] = \frac{\mu_p}{\lambda_s} + \frac{P_{pc}}{\lambda_{ipc}} [1 - e^{-\lambda_{ipc} t_l}] + \frac{P_s}{\lambda_{ix}} [1 - e^{-\lambda_{ix} t_l}] \quad (35)$$

2)  $E[H_2]$ : The UE in this state goes to  $S_1$  only when downlink queue in eNodeB reaches a certain tunable threshold ( $Q_{th}$ ), otherwise, it goes to  $S_3$  or  $S_4$ . The mean holding time in  $S_2$  can be derived as follow:

$$E[H_2] = P_{pc} (\int_0^{t_{ON}} t f_{Q_{th}}(t_{ipc} = t) dt) + \int_{t_{ON}}^{\infty} t_{ON} f_{Q_{th}}(t_{ipc} = t) dt + P_s (\int_0^{t_{ON}} t f_{Q_{th}}(t_{is} = t) dt) + \int_{t_{ON}}^{\infty} t_{ON} f_{Q_{th}}(t_{is} = t) dt \quad (36)$$

3)  $E[H_3]$ : Since any packet arrived during DRX sleep period will be buffered until the next  $t_{ON}$ ,  $E[H_3]$  can be computed as:

$$E[H_3] = t_{ss} = t_{DS} - t_{ON} \quad (37)$$

4)  $E[H_4]$ : Similarly, the mean holding time at state  $S_4$  can be obtained as:

$$E[H_4] = t_{LS} = t_{DL} - t_{ON} \quad (38)$$

After computing the mean holding time and steady-state probabilities, we can now get the expression for the percentage of time that UE spends in DRX sleep cycle, which can be obtained as follows:

$$PS = \frac{\pi_3 E[H_3] + \pi_4 E[H_4]}{\sum_{i=1}^4 \pi_i E[H_i]} \quad (39)$$

For computing average packet delay  $E[D]$ , the Poisson traffic model has been used, that assuming the number of packets that arrive at the eNodeB in a given interval of time follows a Poisson distribution with the average arrival rate  $\lambda$  and variance  $\sigma_A^2 = 1/\lambda^2$ . Thus, the method that has been used in (Herrería-Alonso et al., 2015) and (Christensen et al., 2010) is utilized. Due to the much volume of the average packet delay calculations, here only the average packet delay equation with Poisson traffic is provided. To view, the extraction process can refer to these references. Therefore, we have:

$$E[D] = \frac{1 + \sigma_s^2 \lambda^2 + (1 - \rho)^2}{2\lambda(1 - \rho)} - \frac{Q_{th} - 1}{\lambda Q_{th}} + \frac{(Q_{th} + \lambda T_W)^2 - Q_{th} - 2\lambda(\lambda T_W + t_{DS})}{2\lambda(Q_{th} + \lambda T_W + \gamma - 1)} \quad (40)$$

where  $T_W = \frac{(t_{DS} - t_{ON})^2}{2t_{DS}}$  and  $\gamma = e^{\lambda t_l}$ ,  $\rho$  is the utilization factor ( $\rho = \frac{\lambda}{\lambda_s}$ ) must be less than 1 to assure system stability.  $\sigma_s^2$  is variance of service time demanded by  $n$ -th packet in eNodeB.

#### 4. Performance Evaluation

Java discrete-event simulator was used to obtain the system level simulation results, while MATLAB has been used to obtain the analytical results based on the analytical model proposed in this paper. In the Analytical study, it was first considered that  $t_l$  is constant till the impact of packet queueing in eNodeB until the  $Q_{th}$  threshold to be investigated. Then by using of MATLAB, the best possible value for the  $\alpha$  and  $\beta$  was found. Details of performance evaluation parameters are provided in Table 2.

**Table 2:** Performance Evaluation Parameters

Parameter	Value
$[\lambda_{ip}, \lambda_{ipc}, \lambda_{is}, \lambda_s]$	$[10, \frac{1}{10}, \frac{1}{2000}, 10]$
$[\mu_{pc}, \mu_p]$	$[5, 5]$
$[PSF, t_{ON}, t_I, N_{DS}]$	$[1ms, 100ms, 10ms, 10]$

**A. Analytical Results**

The impact of the short/long sleep period on power saving is illustrated in Fig. 3 and Fig. 4. Comparing Conventional DRX mechanism and DRX with queue mechanism with queue threshold 10 and 5(10-DRX, 5-DRX) in the percentage of time that UE spends on sleep period, DRX with queue mechanism by increasing  $Q_{th}$  saves significant energy, because of the amount of time that UE spends in sleep cycle increases. As shown in these Figures, with increasing  $T_{SS}$  and  $T_{LS}$ , the power saving also increases.

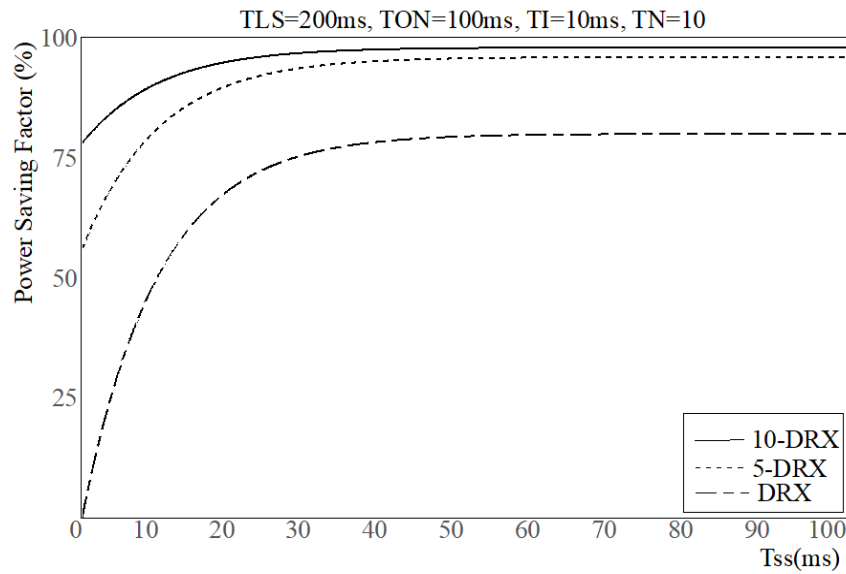


**Figure 3.** Impact of Short Sleep Period on Power Saving for  $Q_{th}$ -DRX and Conventional DRX Mechanism.

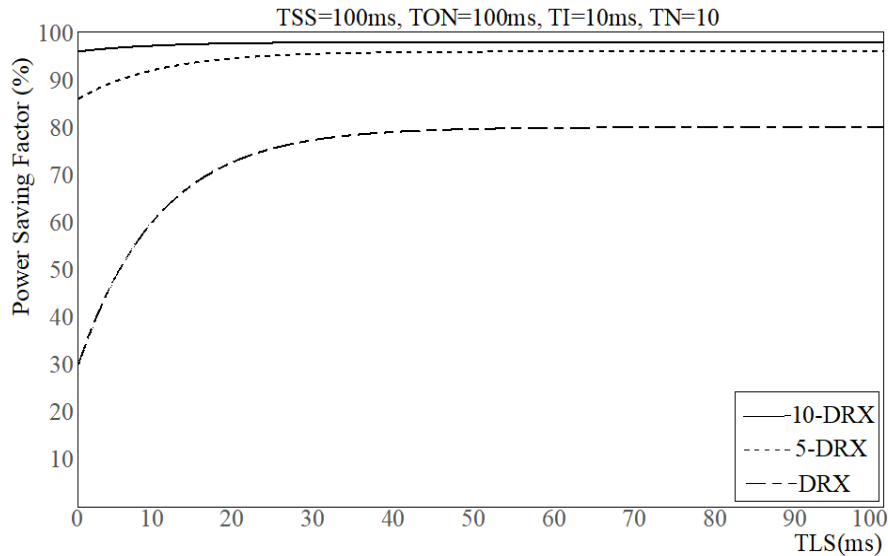


**Figure 4.** Impact of Long Sleep Period on Power Saving for  $Q_{th}$ -DRX and Conventional DRX Mechanism.

The impact of short sleep period on packet delay is illustrated in Fig. 5. It is clear that DRX mechanism with queue threshold ( $Q_{th}$ ) strongly increases packet delay. Because of the eNodeB packet transmission to UE is delayed in DRX mode until its corresponding downlink queue reaches a certain threshold. According to Fig. 5 the use of adaptive algorithm (Algorithm 1) is essential that is able to adjust the queue threshold to real time traffic characteristics with the goal of maintaining average packet delay around a given threshold while keeping energy consumption low enough.

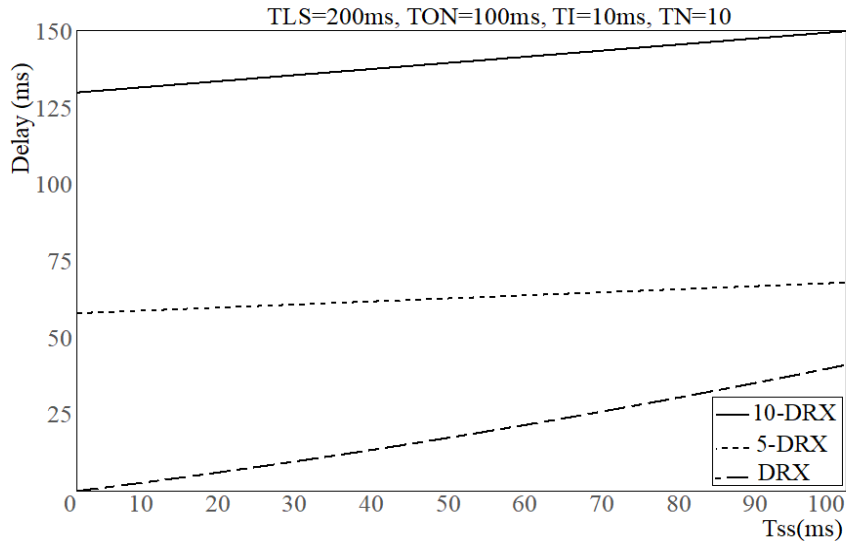


**Figure 5.** Impact of Short Sleep Period on Average Packet Delay for  $Q_{th}$ -DRX and Conventional DRX Mechanism

To get an appropriate value for  $\alpha$  and  $\beta$ , power saving factor is calculated and average packet delay based on two parameters  $\alpha$  and  $\beta$  are measured. Then by using MATLAB, it was tried to maximize power saving factor and at the same time, the average packet delay was minimized. The values obtained for  $\alpha$  and  $\beta$  are considered as optimize values that are used in the simulations.

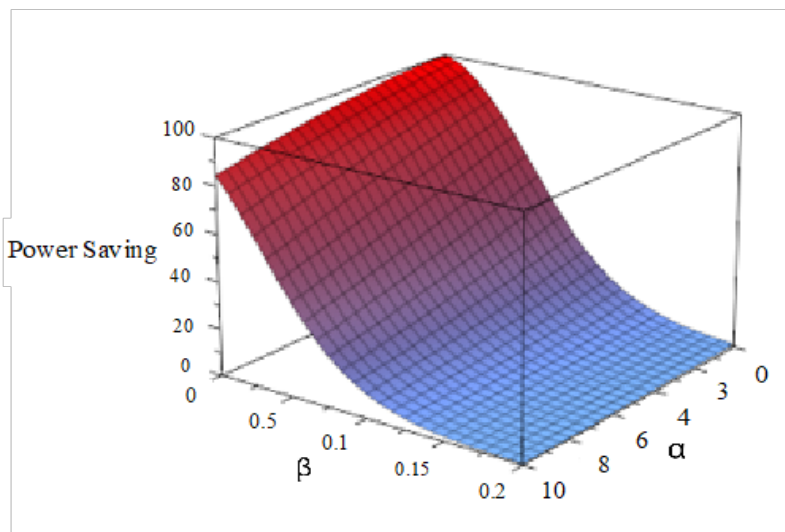


**Figure 6.** Impact of  $\alpha$  and  $\beta$  on Power Saving Factor.

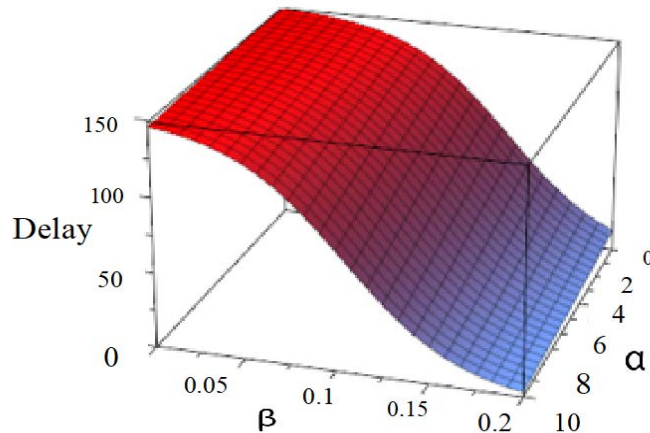


**Figure 7.** Impact of  $\alpha$  and  $\beta$  on Average Packet Delay

As it is observed from Fig. 6 and Fig. 7, with increasing  $\alpha$  and  $\beta$  power saving and average packet delay decreases. For optimal trade-off between power saving and delay,  $\alpha$  and  $\beta$  should be selected based on application's sensitivity to delay.

According to this view for delay sensitive applications  $a$  and  $\beta$  is determined in such a way that maximum possible value of power saving is provided and at the same time average packet delay could not exceed from delay threshold 64ms. In this case  $a=10$  and  $\beta =0.05$  are obtained. For delay tolerant applications we consider delay threshold 512ms and the average packet delay does not exceed from 512ms. In this case  $a=6$  and  $\beta =0.02$  are obtained.

### B. Simulation Results

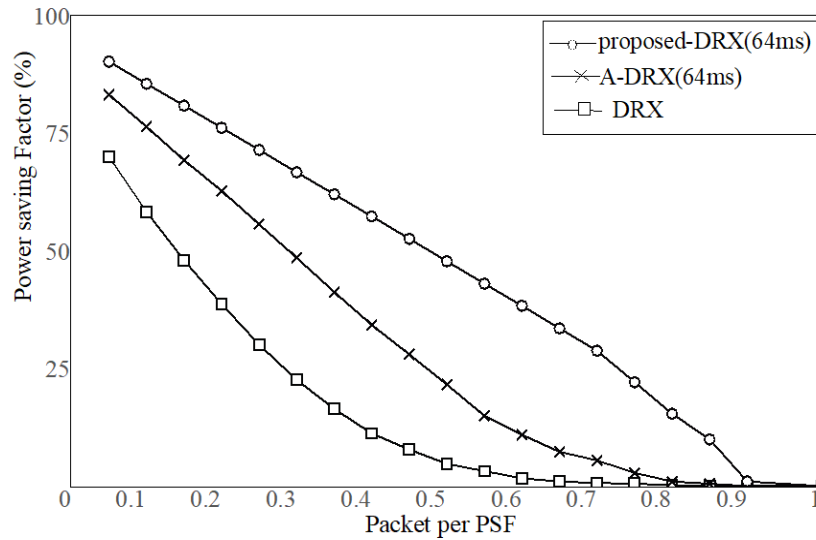
The proposed algorithm was calculated with two different delay thresholds. If the UE is running delay sensitive applications, the delay threshold  $D_{th} = 64\text{ms}$ ,  $a = 10$  is considered and  $\beta = 0.05$ , and if the UE is running delay tolerant applications,  $D_{th} = 512\text{ms}$ ,  $a = 6$  and  $\beta = 0.02$  are chosen. These parameters are summarized in Table 3. To evaluate our algorithm, we have chosen two model traffic. First model is Poisson traffic with an increasing average arrival rate up to 0.9 packets per PSF. Moreover, to test our proposal Under different conditions, we consider Pareto traffic with shape parameter  $a = 1.5$ . In the simulations we consider  $t_{SS} = 32\text{ms}$  and  $t_{LS} = 32\text{ms}$ .

**Table 3:** Simulation Parameters

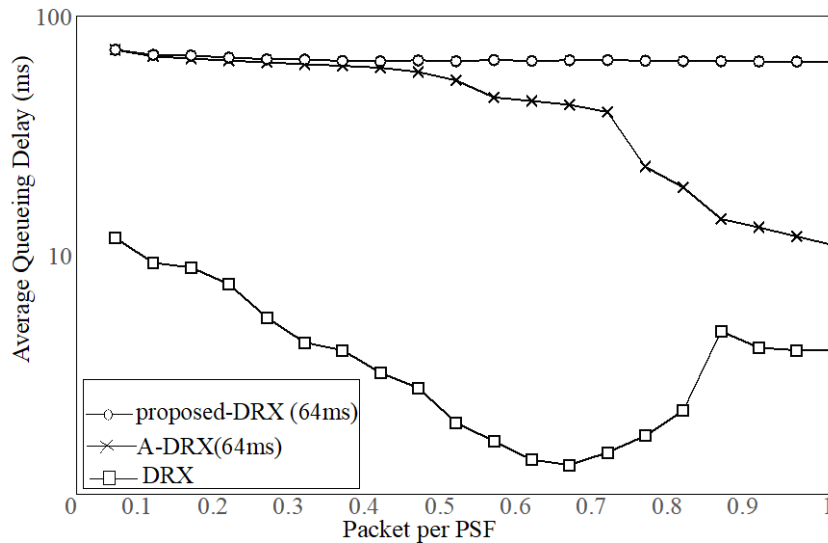
Application Type	Parameter Value
Delay Sensitive	$D_{th} = 64 \text{ ms}$ , $a = 10$ , $\beta = 0.05$
Delay Tolerant	$D_{th} = 512 \text{ ms}$ , $a = 6$ , $\beta = 0.02$

Fig. 8 shows the percentage of time UE spent in the low power mode for conventional DRX (DRX), the Adaptive Coalesced DRX scheme (A-DRX) presented in (Herrería-Alonso et al., 2015) and the proposed algorithm (Proposed-DRX). AS expected, the proposed algorithm was able to save significant energy rather than A-DRX and conventional DRX. In the other words, this algorithm saved more energy with the same delay threshold. The reason is that, when traffic rate is low, consequently  $Q_{th}$  decreases therefore  $t_l$  also decreases to increase power saving in UE and when traffic rate is high,  $Q_{th}$  increases that makes  $t_l$  also increase to decrease delay. For example, in traffic rate 0.4 packet per PSF, power efficiency about 23% compared to A-DRX and about 46% compared to conventional DRX has been increased. Average packet delay for three DRX models are

shown in Fig. 9. Average packet delay in Proposed-DRX and A-DRX in low traffic rate is the same and is in the range of 64ms. As can be seen our algorithm can maintain the average packet delay closer to delay threshold.



**Figure 8.** Energy Saving in three different DRX models with  $D_{th} = 64ms$



**Figure 9.** Average Packet Delay in three different DRX models with  $D_{th} = 64ms$ .

With the higher  $D_{th}$ , the greater energy saving will be obtained, while the packet delay also increases. With increasing traffic rate in  $D_{th} = 512ms$ , our algorithm saves more power than A-DRX scheme, as illustrated in Fig. 10. The delay diagram in case  $D_{th} = 512ms$  is similar to case  $D_{th} = 64ms$ , with this difference that in Proposed-DRX scheme the delay would be in the range of 498ms, which results in much power saving.

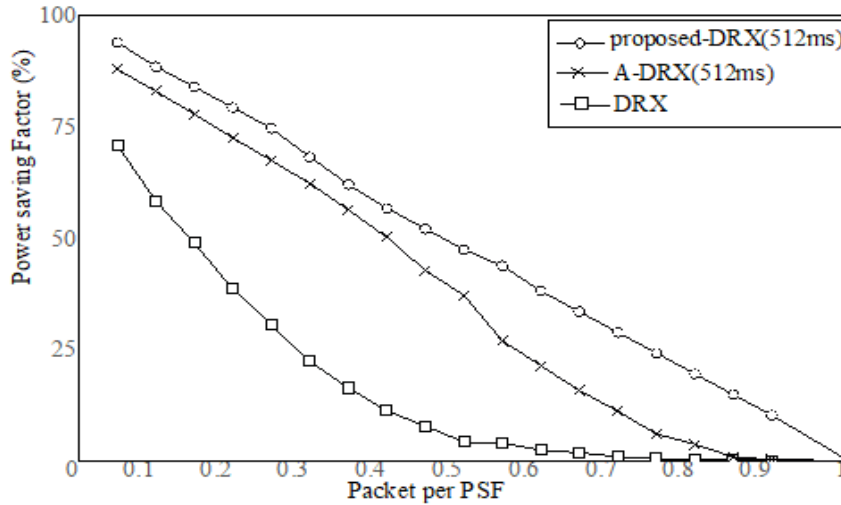


Figure 10. Energy Saving in three different DRX models with  $D_{th} = 512ms$

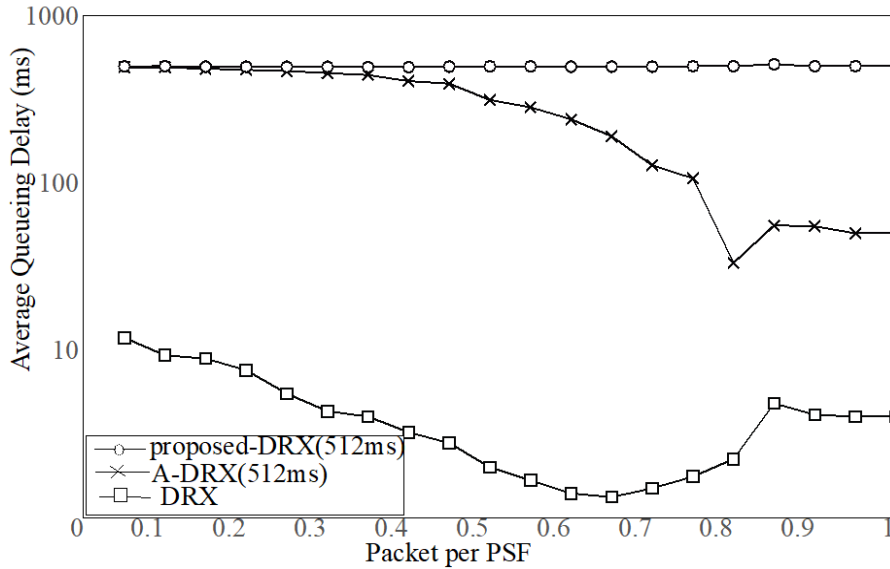


Figure 11. Average Packet Delay in three different DRX models with  $D_{th} = 512ms$ .

### C. Proposed scheme with Self-Similar traffic

In this section to test the performance of our proposed scheme in different traffic characteristic, we conducted several simulations with self-similar traffic. Self-similar traffic such as Internet traffic has truncated-Pareto distribution as defined in 3GPP standard<sup>1</sup>:

$$f(x) = \begin{cases} \frac{\alpha x_m^\alpha}{x^{\alpha+1}}, & x_m \leq x < m \\ \frac{(x_m)^\alpha}{m}, & x = m \end{cases} \quad (41)$$

where  $a$  is the distribution shape parameter, and  $x_m$  is the location parameter. Both of them are positive numbers. For self-similar traffic,  $a$  should be between 1 and 2. Moreover,  $m$  is the value of truncated point

<sup>1</sup> "Feasibility Study for OFDM for UTRAN Enhancement, 3GPP TR 25.892 Std.2.0.0, Rev. 6, 2004.,"



which equals to the maximum value of packet inter-arrival time. In the following simulations we consider the shape parameter  $a= 1.5$ . The results are shown in Fig. 12 and Fig. 13. Fig. 12 shows that our scheme in this traffic model also could achieve greater energy saving compared to the other DRX mechanism. Average packet delay for pareto model is shown in Fig. 13. According to Fig. 13, Proposed- DRX and A-DRX mechanism had the same packet delay but for this same delay our scheme saved more energy. This figure well showed up that proposed DRX scheme for the same delay saved more energy and had higher performance compared to other DRX schemes.

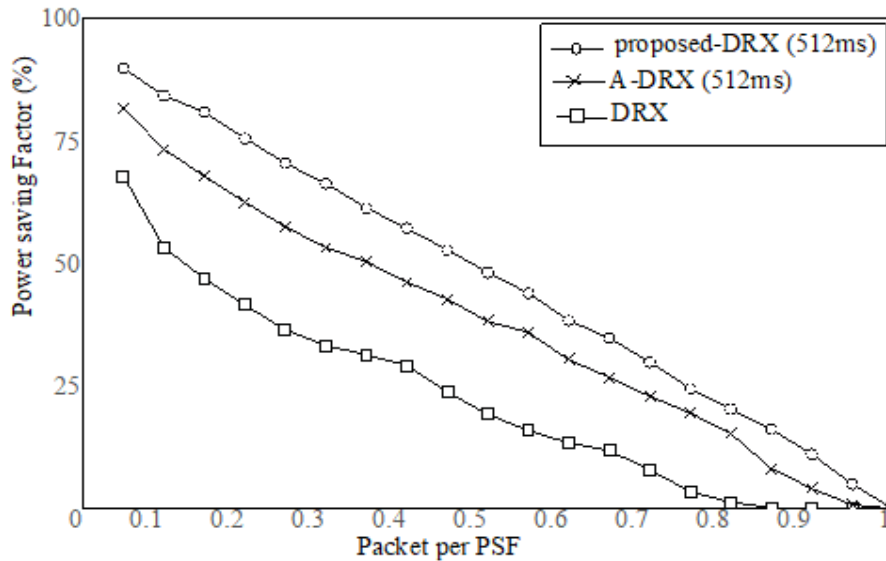


Figure 12. Energy Saving in three different DRX models with Pareto traffic.

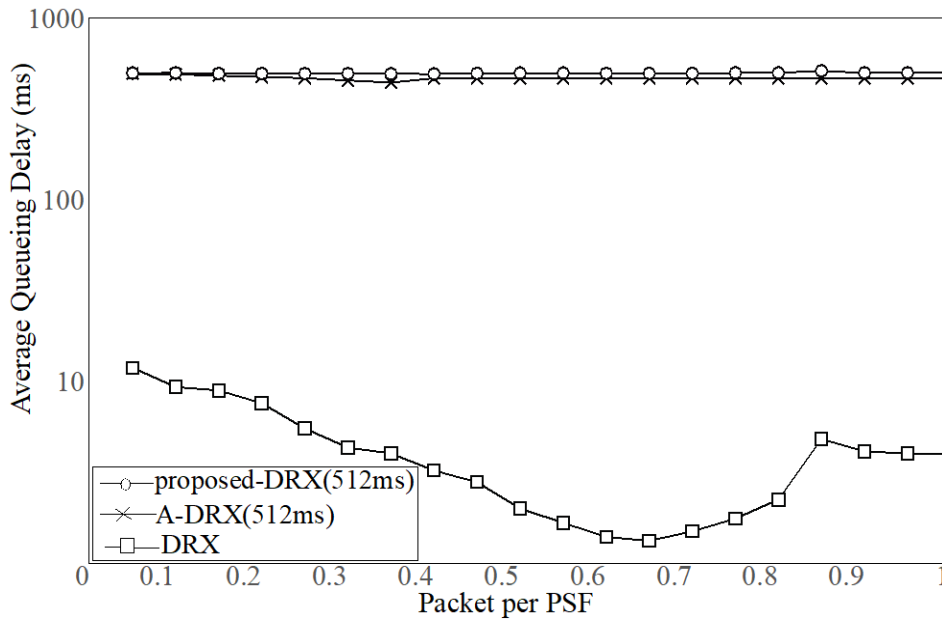


Figure 13. Average Packet Delay in three different DRX models with Pareto traffic.

## Conclusion

In this paper, an adaptive scheme was introduced to optimize the DRX mechanism for reducing energy consumption while maintaining average packet delay around the delay threshold. The algorithm adaptively modified the DRX inactivity-timer according to the traffic rate and queue threshold. The proposed scheme significantly improved the operation of previously developed Adaptive Coalesced DRX mechanism. In Adaptive Coalesced DRX (A-DRX) eNodeBs delay downlink transmission until their downlink queues reached a threshold, thus increasing the amount of time the UEs spent in DRX mode. Our numerical analysis and simulation results showed that proposed scheme was able to achieve significant power saving compared to the other DRX mechanisms

## References

1. Aho, K., Repo, I., Nihtilä, T., & Ristaniemi, T. (2009). "Analysis of VoIP over HSDPA Performance with Discontinuous Reception Cycles," in Information Technology: New Generations, 2009. ITNG'09. Sixth International Conference on, pp. 1190-1194, IEEE.
2. Bontu C. S. and Illidge E., (2009). "DRX Mechanism for Power Saving in LTE," IEEE Communications Magazine, vol. 47, no. 6.
3. Chang, H. L., & Tsai, M. H. (2018) "Optimistic DRX for Machine-Type Communications in LTE-A Network," IEEE Access, vol. 6, pp. 9887-9897.
4. Christensen K., Reviriego P., Nordman B., Bennett M., Mostowfi M., and Maestro J. A., (2010). "IEEE 802.3 az: the Road to Energy Efficient Ethernet," IEEE Communications Magazine, vol. 48, no. 11.
5. Ferng, H. W., & Wang, T. H. (2018). "Exploring Flexibility of DRX in LTE/LTE-A: Design of Dynamic and Adjustable DRX," IEEE Transactions on Mobile Computing, vol. 17, no. 1, pp. 99-112.
6. Fowler S., (2011). "Study on Power Saving Based on Radio Frame in LTE Wireless Communication System Using DRX," in Globecom workshops (gc wkshps), 2011 IEEE, pp. 1062-1066, IEEE.
7. Fowler, S. A., Mellouk, A., & Yamada, N. (2013). LTE-Advanced DRX Mechanism for Power Saving. John Wiley & Sons.
8. Herreria-Alonso, S., Rodriguez-Perez, M., Fernandez-Veiga, M., & Lopez-Garcia, C. (2012). "A GI/G/1 Model for 10 Gb/s Energy Efficient Ethernet Links," IEEE Transactions on Communications, vol. 60, no. 11, pp. 3386-3395.
9. Herreria-Alonso, S., Rodríguez-Pérez, M., Fernández-Veiga, M., & López-García, C. (2015). "Adaptive DRX Scheme to Improve Energy Efficiency in LTE Networks with Bounded Delay," IEEE Journal on Selected Areas in Communications, vol. 33, no. 12, pp. 2963-2973.
10. Iwamura, M., Etemad, K., Fong, M. H., Nory, R., & Love, R. (2010). "Carrier Aggregation Framework in 3GPP LTE-Advanced [WiMAX/LTE Update]," IEEE Communications Magazine, vol. 48, no. 8.
11. Klenrock L., (1975). "Queueing Systems Volume 1: Theory," New York.
12. Lee, M., & Lee, T. J. (2017). "Energy Harvesting Discontinuous Reception (DRX) Mechanism in Wireless Powered Cellular Networks," IET Communications, vol. 11, no. 14, pp. 2206-2213.
13. Liu, Y., Huynh, M., Mangla, A., & Ghosal, D. (2014). "Performance Analysis of Adjustable Discontinuous Reception (DRX) Mechanism in LTE Network," in Wireless and Optical Communication Conference (WOCC), 2014 23rd, pp. 1-6, IEEE.
14. Maheshwari, M. K., Agiwal, M., Saxena, N., & Roy, A. (2017). "Hybrid Directional Discontinuous Reception (HD-DRX) for 5G Communication," IEEE Communications Letters, vol. 21, no. 6, pp. 1421-1424.
15. Ramazanali, H., & Vinel, A. (2016). "Tuning of LTE/LTE-A DRX Parameters," in Computer Aided Modelling and Design of Communication Links and Networks (CAMAD), 2016 IEEE 21st International Workshop on, pp. 95-100, IEEE.

16. Ross S. M., (1996). "Stochastic Processes,"
17. Whinnett, N. W., Tong, F., Xiao, W., & Love, R. T. (2013) "Use of the Physical Uplink Control Channel in a 3rd Generation Partnership Project Communication System," US Patent 8,412,209.
18. Willinger, W., Taqqu, M. S., Sherman, R., & Wilson, D. V. (1997). "Self-Similarity Through High-Variability: Statistical Analysis of Ethernet LAN Traffic at the Source Level," *IEEE/ACM Transactions on Networking (ToN)*, vol. 5, no. 1, pp. 71-86.
19. Xu, S., Liu, Y., & Zhang, W. (2018) "Grouping-Based Discontinuous Reception for Massive Narrowband Internet of Things Systems," *IEEE Internet of Things Journal*, vol. 5, no. 3, pp. 1561-1571.
20. Yang, S. R., Yan, S. Y., & Hung, H. N. (2007). "Modeling UMTS Power Saving with Bursty Packet Data Traffic," *IEEE Transactions on Mobile Computing*, vol. 6, no. 12, 2007.
21. Yu, Y. P., & Feng, K. T. (2012, May) "Traffic-Based DRX Cycles Adjustment Scheme for 3GPP LTE Systems," in *Vehicular Technology Conference (VTC Spring)*, 2012 IEEE 75th, pp. 1-5, IEEE.
22. Zhong, C., Yang, T., Zhang, L., & Wang, J. (2011, September). "A new Discontinuous Reception (DRX) Scheme for LTE-Advanced Carrier Aggregation Systems with Multiple Services," in *Vehicular Technology Conference (VTC Fall)*, 2011 IEEE, pp. 1-5, IEEE.